IEEE Access
Multidisciplinary | Rapid Review | Open Access Journal

Received September 25, 2017, accepted October 11, 2017, date of publication October 16, 2017,
date of current version February 14, 2018.

Digital Object Identifier 10.1109/ACCESS.2017.2763161

12-Port 5G Massive MIMO Antenna Array in Sub-6GHz Mobile Handset for LTE Bands 42/43/46 Applications

YIXIN LI[1], CHOW-YEN-DESMOND SIM[2], (Senior Member, IEEE), YONG LUO[1], AND GUANGLI YANG[1], (Member, IEEE)

[1]School of Communication and Information Engineering, Shanghai University, Shanghai 200444, China
[2]Department of Electrical Engineering, Feng Chia University, Taichung 40724, Taiwan

Corresponding author: Guangli Yang (guangli.yang@shu.edu.cn)

This work was supported by the Shanghai 1000 Talents Plan under Grant SH03027.

ABSTRACT A 12-port antenna array operating in the long term evolution (LTE) band 42 (3400–3600 MHz), LTE band 43 (3600–3800 MHz), and LTE band 46 (5150–5925 MHz) for 5G massive multiple-input multiple-output (MIMO) applications in mobile handsets is presented. The proposed MIMO antenna is composed of three different antenna element types, namely, inverted π-shaped antenna, longer inverted L-shaped open slot antenna, and shorter inverted L-shaped open slot antenna. In total, eight antenna elements are used for the 8×8 MIMO in LTE bands 42/43, and six antenna elements are designed for the 6×6 MIMO in LTE band 46. The proposed antenna was simulated, and a prototype was fabricated and tested. The measured results show that the LTE bands 42/43/46 are satisfied with reflection coefficient better than -6 dB, isolation lower than -12 dB, and total efficiencies of higher than 40%. In addition to that, the proposed antenna array has also shown good MIMO performances with an envelope correlation coefficient lower than 0.15, and ergodic channel capacities higher than 34 and 26.5 b/s/Hz in the LTE bands 42/43 and LTE band 46, respectively. The hand phantom effects are also investigated, and the results show that the proposed antenna array can still exhibit good radiation and MIMO performances when operating under data mode and read mode conditions.

INDEX TERMS Handset antenna, MIMO antenna, sub-6GHz, massive MIMO.

I. INTRODUCTION

As the world is undergoing to embrace the 5G (fifth generation) communication system in the year 2020 or after, new antenna design for 5G base stations and mobile stations will therefore be in great demand in the near future. At present, the 2 × 2 multiple-input multiple-output (MIMO) antenna system for 4G (fourth generation) LTE (long term evolution) wireless communication has already been studied widely and commercialized for mobile handsets [1]. However, it is well known that the 2 × 2 MIMO operating scheme is still incompetent for 5G wireless communication, because 5G is predicted to possess an aggregate data rate of 1,000 times faster than 4G and has better link reliability [2]. As 5G mobile handsets with either 2 × 2 MIMO or 4 × 4 MIMO scheme is only to be applied for 2G/3G/4G (698–960 MHz, 1710–2690 MHz) communication, hence, multiple antenna elements (more than 4) are needed to operate at 5G frequency bands for massive MIMO applications [3]. Compared with the 4G MIMO antenna systems, at least 6 to 8 antenna elements are integrated into a mobile terminal for 5G massive MIMO to provide good diversity gain and multiplexing gain [4]. Through spatial diversity and spatial multiplexing, larger channel capacity and better communication reliability can be achieved. Therefore, the multi-antenna system is much more capable of resisting multipath fading and improving data throughput [5], [6].

As the international standard for 5G communication is now being formulated, the 5G frequency bands are not formally issued at the moment. At the World Radio Communication Conference 2015 (WRC-15), 3400–3600 MHz in the C band was allocated as a new IMT band for future 5G wireless communication [7]. Therefore, frequency bands below 6 GHz that are also known as sub-6GHz bands are presently a topic of concern to all countries. Presently, the

3400–3800 MHz band, which is the combination of LTE band 42 (3400–3600 MHz) and LTE band 43 (3600–3800 MHz) has been recognized by many countries as a pioneer to realize 5G massive MIMO. For example, the European Union (EU) has decided to preferentially develop the 3400–3800 MHz band [8], while China has also started to investigate 3400–3600 MHz band as 5G and sub-6GHz band [9], and Korea has selected 3400–3700 MHz band for their preliminary study [10]. However, LTE bands 42/43 are not sufficient for the upcoming 5G multiband communication. To further support more potential sub-6GHz frequency bands, LTE band 46 (5150–5925 MHz), which is also known as an unlicensed band (LTE-unlicensed, LTE-U) restricted to licensed-assisted access operation (LTE-Licensed Assisted Access, LTE-LAA) [11], is also to be taken into account for 5G massive MIMO antenna design.

Several mobile terminal antennas designed for sub-6GHz massive MIMO have been reported [12]–[14]. An 8-element antenna array for LTE band 42 has been studied in [12], and its measured ergodic channel capacity (for a 2 × 8 MIMO channel) has reached approximately 16 bps/Hz with a 20-dB signal-to-noise ratio (SNR). However, the antenna elements are placed along all the four edges of a handset, and no other available spaces are reserved for the 4G antennas. In [13], a 10-antenna array operating at LTE bands 42/43 has been investigated, and its measured peak ergodic channel capacity with 20-dB SNR was 47 bps/Hz. Interestingly, the work in [14] has presented an 8-port MIMO antenna array working at 2.6-GHz band with orthogonal polarization characteristic, and its channel capacity can reach up to 40 bps/Hz with 20-dB SNR for an 8 × 8 MIMO antenna system. Some other massive MIMO antennas have also been reported for mobile handsets [15]–[19]. However, the impedance bandwidths of these referenced antennas are still not wide enough to cover the LTE band 46 as a sub-6GHz band for the forthcoming LTE-U and LTE-LAA massive MIMO applications. In addition, even though there is enough space at two corners located along the short edges of the printed circuit board (PCB), which is usually reserved for 2G/3G/4G 2 × 2 MIMO antennas in some of the references mentioned in [15]–[19], the other two corners of the PCB are not fully exploited for MIMO operation. Therefore, it is still challenging for antenna engineers to design a massive MIMO antennas that can cover more sub-6GHz bands, which include LTE bands 42, 43 and 46, along with desirable inter-element isolation and antenna efficiency.

In this paper, a novel 12-port dual-band massive MIMO antenna array that can cover both the 3400–3800 MHz (LTE bands 42/43) and 5150–5925 MHz (LTE band 46) for future 5G mobile handsets is proposed. Here, twelve antenna elements are integrated into the PCB of the handset, and amid these antenna elements, three different antenna types, namely, inverted π-shaped antenna (IA), longer inverted L-shaped open slot antenna (LA) and shorter inverted L-shaped open slot antenna (SA) are disposed at different locations with different excited operating frequency bands. The proposed MIMO antenna array is simulated, fabricated and measured.

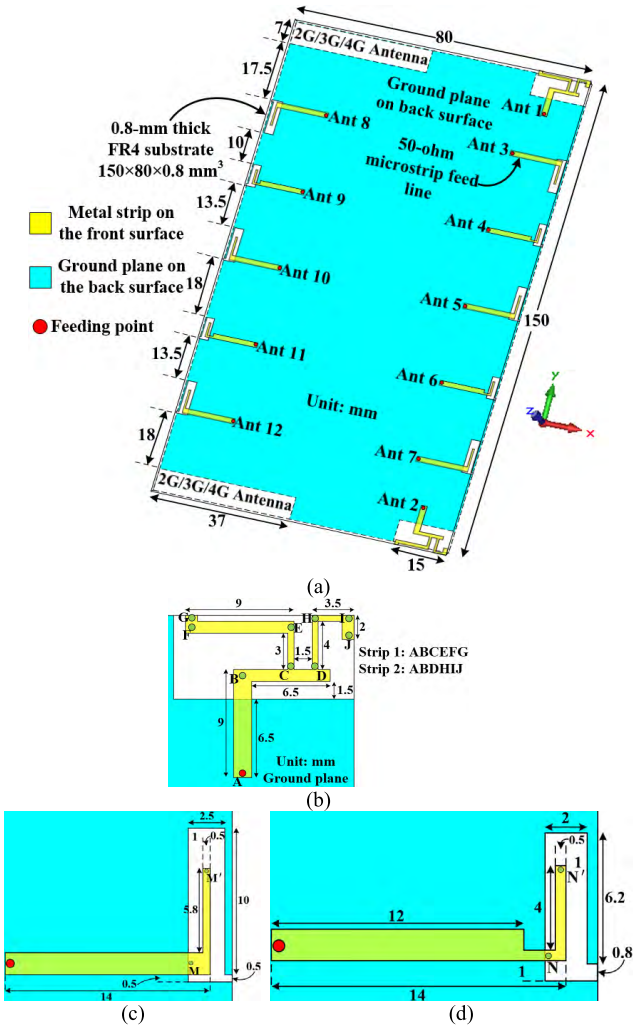

FIGURE 1. Geometry and detailed dimensions of the proposed 12-antenna array. (a) Overall view, (b) Inverted π-shaped antenna (IA), (c) Longer inverted L-shaped open slot antenna (LA), (d) Shorter inverted L-shaped open slot antenna (SA).

The simulated results are obtained through CST Microwave Studio version 15. The S-parameters and antenna efficiencies are measured using Agilent vector network analyzer E5071C and ETS microwave anechoic chamber, respectively. The ECC and ergodic channel capacity are calculated from the measured results. The effects of the ground plane size on the antenna performances are also studied [20], [21]. It is found that the modification of the ground plane brings some effects on the antenna matching and isolation. However, as the ground plane size for a certain smartphone is fixed, the ground plane effects are not discussed in this paper.

II. PROPOSED MIMO ANTENNA ARRAY

A. ANTENNA STRUCTURE

Fig. 1 shows the detailed structure of the proposed 12-element antenna array for sub-6GHz smartphone applications. Fig. 1(a) depicts the overall geometry of the proposed multiple-input multiple-output (MIMO) antenna array. Here, all the antenna elements are printed on the front surface

of a FR4 dielectric substrate (relative permittivity 4.4 and loss tangent 0.02.) of dimension 150 mm × 80 mm × 0.8 mm, which is typical size for smartphones with 5.7-inch display. The antenna's system ground plane (150 mm × 80 mm) is printed on the back surface of the FR4 substrate, and two rectangular clearance regions of size 7 mm × 37 mm are reserved for the 2G/3G/4G MIMO antennas (main and diversity). If the clearance region is moved to the middle section, it only has negligible effects to the antenna elements, and for brevity, these effects are not studied. As for the other two rectangular clearance regions of size 7 mm × 15 mm printed on top right and bottom right corners of the FR4 substrate, they are for disposing the two IAs (Ants 1 and 2) designated to excite dual-band operation that can cover the long term evolution (LTE) bands 42/43 and LTE band 46. To realize massive MIMO at these two LTE bands, six LAs (Ants 3, 5, 7, 8, 10, 12) operating at LTE bands 42/43 and four SAs (Ants 4, 6, 9, 11) operating at LTE band 46 are also placed along the two side edges of the system ground plane. Owing to the staggered arrangement of the two types of open slot antennas, good isolation and envelope correlation coefficient (ECC) can be achieved, and better spatial diversity performance is also acquired. Therefore, one can see that the proposed twelve antenna elements can form an 8 × 8 MIMO antenna array (Ants 1, 2, 3, 5, 7, 8, 10, 12) for LTE bands 42/43, and a 6 × 6 MIMO antenna array (Ants 1, 2, 4, 6, 9, 11) for LTE band 46. Thus, the proposed antenna is capable of achieving massive MIMO operation not only in traditional LTE bands 42/43, but also in up-to-date LTE band 46 for 5G communication.

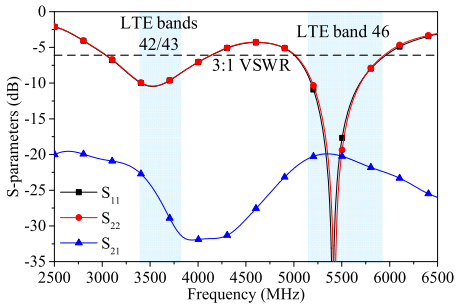

FIGURE 2. Simulated S-parameters of IAs (Ants 1 and 2).

B. INVERTED π-SHAPED ANTENNA (IA)

Fig. 1(b) shows the detailed geometry and dimensions of the IA, which is a dual-branch monopole antenna fed at point A via a 50-ohm microstrip feedline. The IA is mainly composed of two branch strips, namely, strip 1 (with path ABCEFG) that generates one-quarter-wavelength fundamental mode at around 3.5-GHz to cover LTE bands 42/43, and strip 2 (with path ABDHIJ) that generates its high-order mode at approximately 5.5-GHz to fully cover LTE band 46. Thus, each strip generates a resonant mode, and the two modes can be combined to cover both LTE bands 42/43 and LTE band 46. Fig. 2 shows the simulated reflection coefficients of Ant 1 (S_{11}) and Ant 2 (S_{22}), and their corresponding isolation (S_{21}). In this figure, the two resonant modes excited by the proposed IA can fully support both the LTE bands 42/43 and LTE band 46 with reflection coefficient better than −6 dB (3:1 voltage standing wave ratio, VSWR). Here, because Ants 1 and 2 are identical in their structures, the reflection coefficients (S_{11} and S_{22}) are in very good agreement, which is a desirable feature for practical applications. Furthermore, because Ants 1 and 2 are disposed at the two corners of the system ground plane (distance between them is 123 mm), good spatial diversity is therefore attained, leading to good isolation (S_{21}) of lower than −20 dB within the two bands of interest.

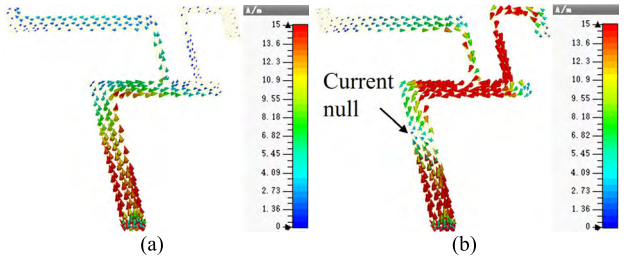

FIGURE 3. Surface current density distributions of Ant 1. (a) Strip 1 at 3500 MHz, (b) Strip 2 at 5500 MHz.

To clearly demonstrate the two resonant modes, Fig. 3(a) and (b) show the surface electric current density distributions of one of the IAs (Ant 1) at 3500 MHz and 5500 MHz, respectively. At 3500 MHz, a quarter-wavelength current distribution at path BCEFG can be observed along strip 1. As strip 1 is a monopole antenna type, thus, this mode is considered as a fundamental mode of strip 1. In contrast, at 5500 MHz, two current nulls (first null at path AB, and second null at point J) on strip 2 are observed, and current changes its direction at the first null (at path AB). As strip 2 is also a monopole type, this current distribution indicates that the 5.5-GHz resonant mode is the first higher-order mode of strip 2 [22], [23].

C. INVERTED L-SHAPED OPEN SLOT ANTENNAS (LA AND SA)

Figs. 1(c) and 1(d) show the detailed geometry and dimensions of the two inverted L-shaped open slot antennas (LA and SA) resonating at approximately 3.6-GHz and 5.5-GHz, for LTE bands 42/43 and LTE band 46, respectively. Both open-slot antennas are etched on the back surface of the FR4 substrate, and fed by an inverted-L shaped microstrip feedline printed on the front surface. Notably, the two open slots are folded into an inverted-L shape type to minimize the size of the antenna elements. By adjusting the length and width of MM′ and NN′ (vertical section of the feeding line), the two open slot antennas can be well excited, tuned and matched. The LA and SA have dimensions of 10.5 mm × 3 mm (0.126 λ × 0.036 λ, where λ is the wavelength at 3.6-GHz) and 7 mm × 2.5 mm (0.117 λ × 0.042 λ, where λ is the wavelength at 5.5-GHz),

respectively. Even though it is well known that the fundamental resonant mode of an open slot antenna (or slot monopole) is at one quarter-wavelength [24], however, in this work, the lengths of the two open slots are only 0.126 λ and 0.117 λ, which are far smaller than a quarter-wavelength at 3.6 GHz and 5.5 GHz, and the widths thereof are merely 3 mm and 2.5 mm, respectively. Thus, the proposed open slot antenna elements are very small in size and can fit into narrow frames in modern smartphones with large screens.

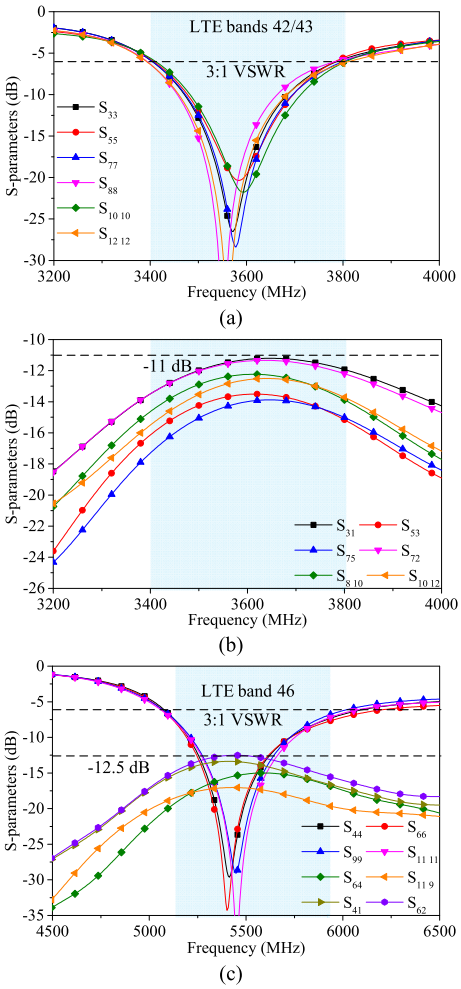

FIGURE 4. Simulated S-parameters. (a) Reflection coefficients of the 3.6-GHz LAs (for Ants 3, 5, 7, 8, 10, 12), (b) Isolations (between adjacent ports) with respect to the IAs (Ants 1, 2) and 3.6-GHz LAs, (c) Reflection coefficients and isolations of the 5-GHz SAs (Ants 4, 6, 9, 11).

Fig. 4(a) shows the simulated reflection coefficients of the 3.6-GHz LAs (for Ants 3, 5, 7, 8, 10, 12). In this figure, all LAs can support the LTE bands 42/43 with reflection coefficient lower than −6 dB. Fig. 4(b) shows its corresponding isolations (between adjacent ports) with respect also to the 3.6-GHz IAs (Ants 1, 2) and 3.6-GHz LAs. As shown in this figure, the isolations of any two 3.6-GHz LAs (S_{53}, S_{75}, S_{810}, S_{1012}) are better than −12 dB. In addition, the isolations between two different 3.6-GHz antennas, namely LAs and IAs (S_{31} and S_{72}), are still better than −11 dB. The simulated reflection coefficients and isolations of (four out of six) the 5-GHz SAs (Ants 4, 6, 9, 11) are presented in Fig. 4(c). Here, the 5-GHz SAs can well cover the LTE band 46 with reflection coefficient lower than −6 dB as well. The corresponding isolations (such as S_{64} and S_{119}), including isolations of different antenna types (S_{41} and S_{62}), are better than −12.5 dB. From the above simulated results, it can be concluded that the staggered configuration of the two open slot antennas (LAs and SAs) can yield satisfactory isolation performances (lower than −11 dB and −12.5 dB in LTE bands 42/43 and in LTE band 46) even if all the antenna elements are unbalanced electric and magnetic monopoles disposed in a very compact space along the longer and the shorter edges of the system PCB.

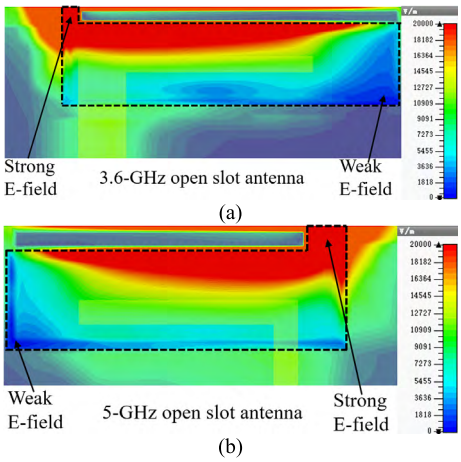

FIGURE 5. Simulated surface electric field distribution of the two open slot antennas (LA and SA), respectively, at (a) 3600 MHz, (b) 5500 MHz.

To further verify the resonant modes of the two proposed open slot antennas (LA and SA), surface electric field (E-field) distributions along the slot surface at 3600 MHz (for LA) and 5500 MHz (for SA) are simulated, and the results are shown in Fig. 5(a) and (b), respectively. It is observed that for both open slot antennas, the surface E-field shows its peak value at the open portion and zero at the short-circuited portion. This behavior is reasonable, as the open portion is of the maximum impedance and the short circuited portion is of the minimum impedance [25]. Moreover, from the view of boundary conditions, the open slot antenna is also a magnetic monopole that can be regarded as the hemisection along the magnetic wall of traditional half-wavelength closed slot antennas, i.e., magnetic dipole. Because of the fact that cutting along the magnetic wall does not vary the boundary conditions along the slot, by removing another identical half slot along the magnetic wall, i.e., the open-circuit plane, the electric field distribution within the slot remains unchanged [26]. Furthermore, the surface E-field propagates one quarter-wavelength from open portion to short-circuited portion, indicating that both the proposed open slot antennas operate at one quarter-wavelength magnetic monopole mode.

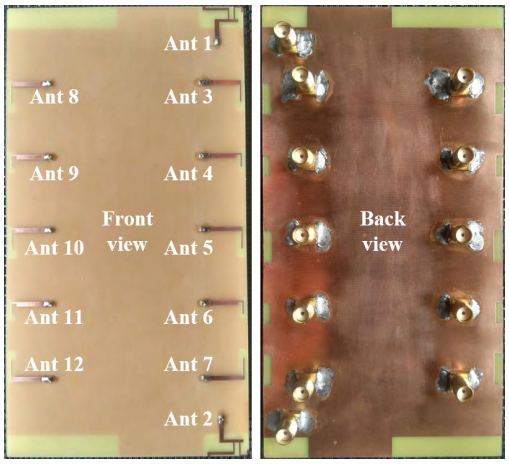

FIGURE 6. Photographs of the fabricated prototype.

III. RESULTS AND DISCUSSION

The proposed 12-element 5G MIMO antenna array was fabricated and tested, and the photos from the front view and the back view are shown in Fig. 6. The feeding points of all 12-element are directly connected to 50-ohm Sub-Miniature-A (SMA) connectors via the ground plane. The measured results and performance metrics of this 12-element 5G MIMO antenna array are shown and discussed in the following sub-sections.

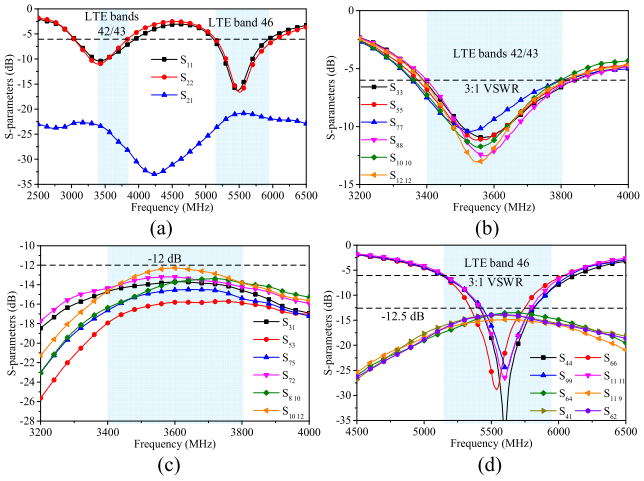

FIGURE 7. Measured S-parameters. (a) Reflection coefficients and isolation of the dual-band IAs (for Ants 1, 2), (b) Reflection coefficients of the 3.6-GHz LAs (for Ants 3, 5, 7, 8, 10, 12), (c) Isolations (between adjacent ports) of the 3.6-GHz IAs and 3.6-GHz LAs, (d) Reflection coefficients and isolations of the 5-GHz SAs and 5-GHz IAs.

A. S-PARAMETERS

The measured S-parameters of the fabricated antenna prototype are given in Fig. 7. In this figure, it is observed that the measured results are in good agreement with the simulated ones shown in Fig. 4. The slight differences between the two results are maybe due to the insertion loss of the SMA connector, and slight fabrication inaccuracy/tolerance. Fig. 7(a) shows the reflection coefficients and isolation of the dual-band IAs (for Ants 1 and 2). Here, Ants 1 and 2 have exhibited good −6 dB impedance bandwidths of 23.3% (3040–3840 MHz) and 15% (5114–5946 MHz), respectively, which can well cover the LTE bands 42/43 and LTE band 46, and their corresponding isolation (S_{21}) is better than −20 dB.

The measured reflection coefficients of the 3.6-GHz LAs (for Ants 3, 5, 7, 8, 10, 12) are shown in Fig. 7(b). Here, the minimum −6 dB impedance bandwidth was 12.1% (3400–3838 MHz), which can cover LTE bands 42/43. As for its corresponding isolations between the adjacent ports of the 3.6-GHz IAs and 3.6-GHz LAs, Fig. 7(c) shows that they are well below −12 dB. The measured reflection coefficients and isolations of (four out of six) the 5-GHz SAs (Ants 4, 6, 9, 11) are presented in Fig. 7(d). Here, the minimum −6 dB impedance bandwidth was 16% (5154–6050 MHz), which can well cover the LTE band 46. As for its corresponding isolations (S_{64} and S_{119}), including those of different antenna types (S_{41} and S_{62}), they are better than −12.5 dB. In summary, the measurement results indicate that the proposed MIMO array antenna can fully cover both LTE bands 42/43 and LTE band 46 with good reflection coefficients and isolation performances.

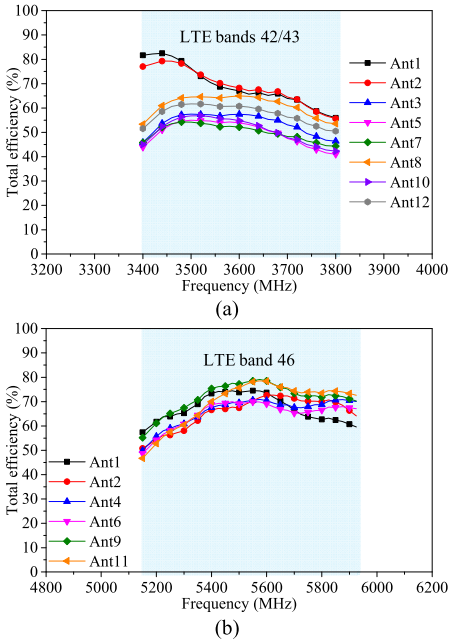

FIGURE 8. Measured total efficiency in (a) LTE bands 42/43, (b) LTE band 46.

B. RADIATION PERFORMANCES

The total efficiencies of the 8 × 8 MIMO and 6 × 6 MIMO antenna elements were measured, and its corresponding results are shown in Figs. 8(a) and (b), respectively. It is worth noting that the total efficiencies measured in here have included the radiation, mismatching and mutual coupling losses. The results are obtained under the circumstance that

one antenna element is excited while all the other elements are connected to 50-ohm matched loads. As shown in these two figures, the measured total efficiencies for LTE bands 42/43 varied approximately between 41% and 82%. As for the measured total efficiencies for LTE band 46, they have varied approximately between 47% and 79%.

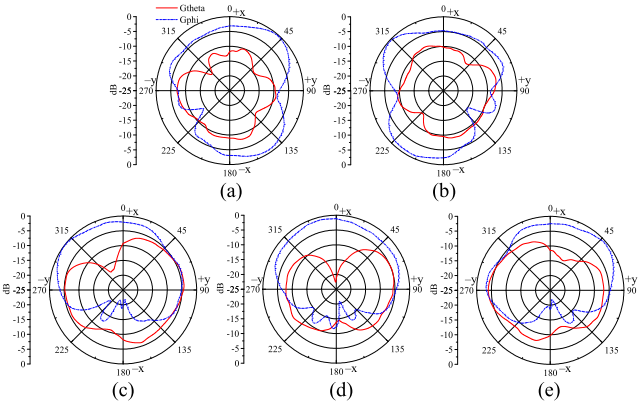

FIGURE 9. Measured radiation patterns of proposed antenna at 3600 MHz. (a) Ant 1, (b) Ant 2, (c) Ant 3, (d) Ant 5, (e) Ant 7.

The measured theta-polarized and phi-polarized realized gain patterns in the xoy plane of the proposed MIMO array antenna at 3600 MHz (for 8 × 8 MIMO) and 5500 MHz (for 6 × 6 MIMO) are shown in Figs. 9 and 10, respectively. For brevity, only the results of Ants 1 to 7 are given. As shown in Fig. 9, Ants 1 and 2 have demonstrated strong radiation in phi = 45° and phi = 315° directions, thus yielding good radiation diversity. In addition to that, the main lobes of Ants 3, 5, and 7 have also shown strong radiation in the +x axis direction, which can be seen at near phi = 315°, phi = 0°, and phi = 45°, respectively.

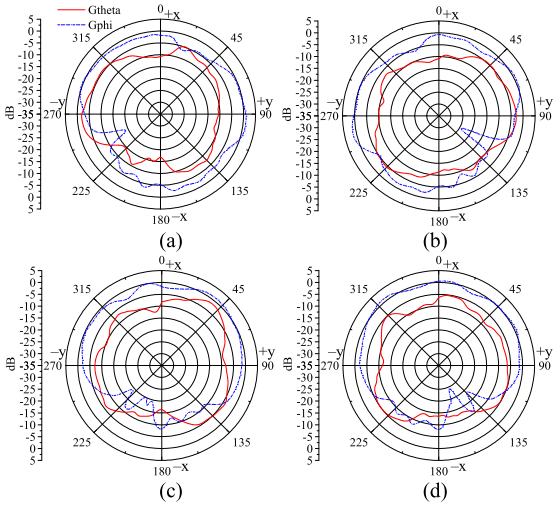

FIGURE 10. Measured radiation pattern of the proposed antenna at 5500 MHz. (a) Ant 1, (b) Ant 2, (c) Ant 4, (d) Ant 6.

As depicted in Fig. 10, at 5500 MHz, Ants 1 and 2 have shown maximum radiation oriented in −y and +y directions, while Ants 4 and 6 are radiating nearly towards phi = 45° and phi = 315° directions, respectively. In summary, the two IAs and the open slot antennas (LAs and SAs) have shown distinguishing and complementary patterns with maximal radiation orientations scattered, which is a good feature for obtaining good spatial/radiation diversity performances. Furthermore, both LAs and SAs have exhibited relatively weaker radiation at near −x axis direction. This is reasonable as the isolations between LAs and SAs that are placed along the left and right side edges are very high.

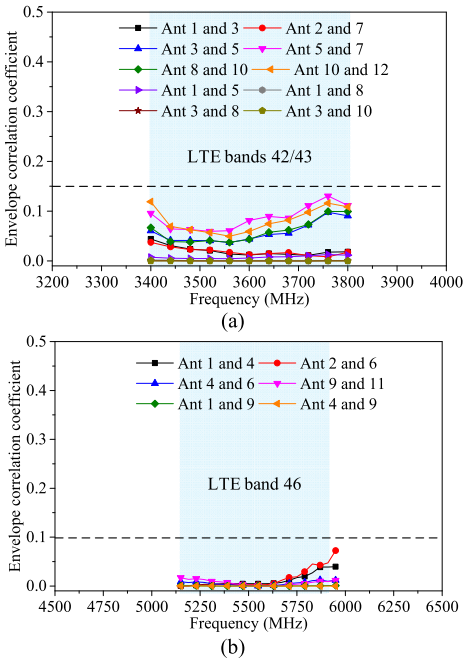

FIGURE 11. Calculated envelope correlation coefficient (ECC) values from the measured results in (a) LTE bands 42/43, (b) LTE band 46.

C. MIMO PERFORMANCES

Since the MIMO antenna array mainly works for diversity and multiplexing applications, besides reflection, isolation and radiation performances, it is quite important to investigate the diversity and multiplexing performances. The envelope correlation coefficients (ECCs) of diverse antenna pairs are studied in this subsection to evaluate and validate the diversity performance of the proposed MIMO antenna array. The exact formula that is used to compute the ECC has been explicitly explained in [27]. Fig. 11 shows the ECCs of the proposed MIMO antenna array calculated from the measured complex electric field results. In this figure, it is observed that the calculated ECC values were lower than 0.15 and 0.1 in the LTE bands 42/43 and LTE band 46, respectively, which is well better than the acceptable criterion of ECC less than 0.5. As lower ECC values will results in higher diversity gain, it can be inferred that the proposed MIMO antenna array has desirable diversity capability.

To verify the multiplexing performances under high SNR, and also to figure out the data transmitting rate potential of the

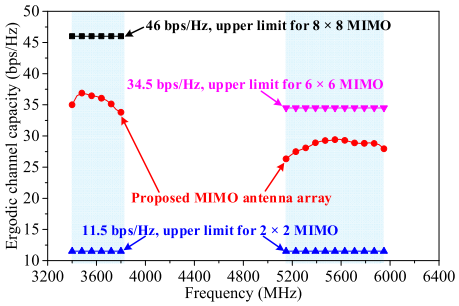

FIGURE 12. Calculated ergodic channel capacity from measured results.

proposed MIMO antenna system under specific propagation scenario, the ergodic channel capacity is therefore studied in here. If the transmitter does not know the channel state information (CSI) and the transmit power is equally allocated to every transmit antenna, the ergodic channel capacity can be achieved by the formula given in [28]. Here, the ergodic channel capacity is obtained by assuming an independent and identically distributed (i.i.d.) Rayleigh fading channel of 20-dB SNR in the propagation environment, and the elements of spatially white channel matrix are independent zero mean circularly symmetric complex Gaussian (ZMCSCG) random variables with unit variance. By averaging 100,000 random i.i.d. 8×8 and 6×6 Rayleigh fading channel realizations for LTE bands 42/43 and LTE band 46, the ergodic channel capacities calculated from measured results in the desired bands of interest are obtained. As shown in Fig. 12, the proposed MIMO array antenna achieves channel capacity of 34–37 bps/Hz and 26.5–29.5 bps/Hz in the LTE bands 42/43 and LTE band 46, respectively. The peak ergodic channel capacities of the proposed MIMO array antenna are approximately 321.7% and 256.5% better than the upper capacity boundary for 2×2 MIMO (at 11.5 bps/Hz). Notably, although the capacity is restricted by the MIMO order for LTE band 46, very high data throughput can still be acquired in this band as well, because the absolute bandwidth of LTE band 46 (775 MHz) is about four times of the absolute bandwidth (200 MHz) of LTE bands 42 and 43. As a whole, the proposed antenna provides much greater multiplexing capability than traditional 4G low-order MIMO.

D. HAND PHANTOM EFFECTS

In this sub-section, the effects of hand phantoms on the performances of the proposed MIMO antenna array are studied. Here, the hand phantom effects are analyzed under data mode (single-hand mode) and read mode (double-hands mode, RM). For data mode, both right hand mode (RHM) and left hand mode (LHM) are studied. The corresponding three application scenarios for hand operation are given in Fig. 13.

Figs. 14(a), (b), and (c) show the simulated total efficiency results under the RHM, LHM and RM, respectively. As shown in Fig. 14(a), for the RHM in the LTE bands 42/43, Ants 2 and 12 have shown good radiation performances with

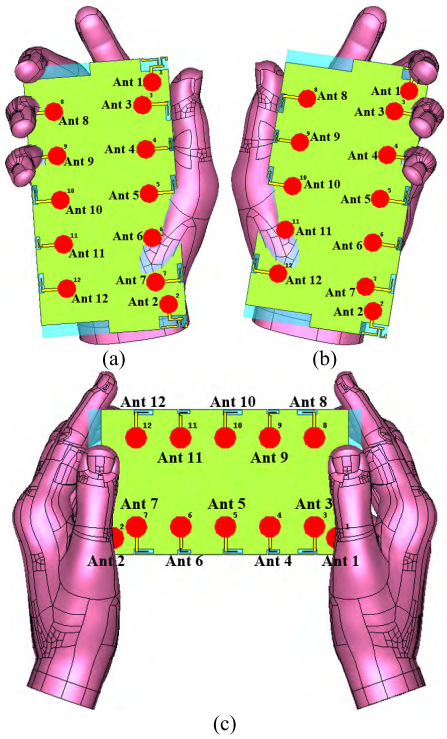

FIGURE 13. Three typical application scenarios under user's hand operation. (a) Right Hand Mode (RHM), (b) Left Hand Mode (LHM), (c) Read Mode (RM).

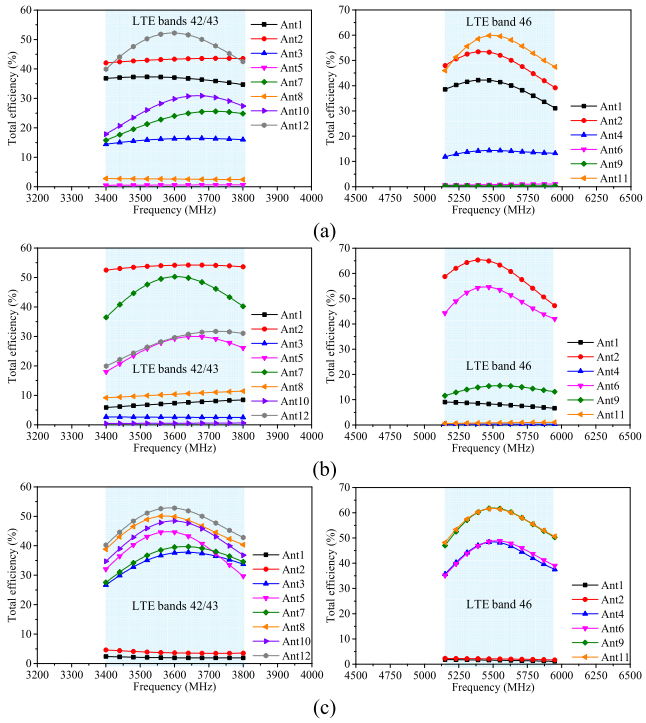

FIGURE 14. Simulated total efficiency under (a) RHM, (b) LHM, (c) RM.

total efficiencies better than 40%, and total efficiency of Ant 1 is still higher than 30%. As for its corresponding RHM working in the LTE band 46, Fig. 14(a) has also shown that

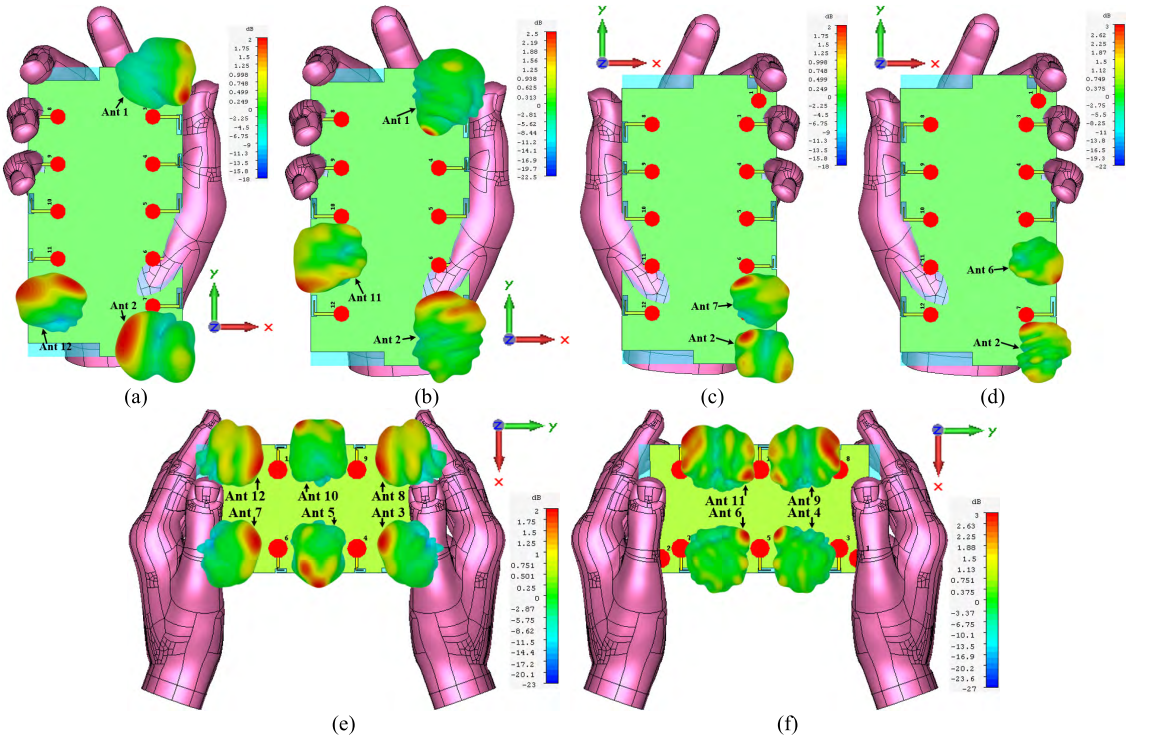

FIGURE 15. Simulated gain patterns of the proposed MIMO antenna array under (a) RHM, 3600 MHz, (b) RHM, 5500 MHz, (c) LHM, 3600 MHz, (d) LHM, 5500 MHz, (e) RM, 3600 MHz, (f) RM, 5500 MHz.

Ants 1 and 2 still work well with total efficiencies higher than 30% and 40%, and the total efficiency of Ant 11 is better than 40%. Nevertheless, the total efficiencies of other antenna elements have deteriorated tremendously, in which this behavior is highly relative to the nature of the hand tissue and the locations of the five fingers with respect to the individual antenna elements. This is because the hand tissue is a very lossy medium, and thus the power radiated from the antenna elements will be absorbed, especially when the open portions (with maximum electric field values) of the open slot antennas (LAs or SAs) are covered by the hand (or fingers) [29], [30].

Although the antenna elements that are in close proximity to hand phantom will experience deteriorated performances, the antenna elements that are a little farther from the hand phantom, i.e., Ants 1, 2, 12 for LTE bands 42/43 and Ants 1, 2, 11 for LTE band 46, are still resistant to hand operation. Under the LHM condition, the hand phantom is a mirror image of the RHM condition, in which the antenna array is keeping still in the same position. As shown in Fig. 14(b), because Ant 1 is covered by the hand, thus its efficiency has dropped to below 10% in LTE bands 42/43 and LTE band 46. However, the total efficiencies of Ants 2, 7 at LTE bands 42/43 and Ants 2, 6 at LTE band 46 are generally higher than 40%.

At RM condition, because only Ants 1 and 2 are covered by the hand phantom, therefore, as shown in Fig. 14(c), only Ants 1 and 2 are showing much deteriorated total efficiencies of lower than 5%. In contrast, because the open slot antennas (LAs and SAs) that are disposed along the two side edges of the PCB are not covered by the hand phantom, they have shown better total efficiencies than the LHM and RHM ones. By further observing Fig. 14(c), in the LTE bands 42/43 and LTE band 46, total efficiencies of better than 25% and 35% are observed, respectively. From the above results, one can still see that the proposed antenna array can still work for MIMO applications, even when most of the array elements are covered by lossy hand tissue under data mode.

To illustrate the spatial diversity characteristic with the presence of hand phantoms, the antenna gain patterns at 3600 MHz and 5500 MHz under data mode and read mode are simulated, and the results are given in Fig. 15. Under RHM condition, the proposed MIMO antenna array mainly works at 3 × 3 MIMO scenario, with Ants 1, 2, 12 operating at LTE bands 42/43 and Ants 1, 2, 11 operating at LTE band 46, as shown in Figs. 15(a) and (b), respectively. At 3600 MHz, Ants 1, 2, 12 mainly radiate towards +x, −x, +y directions, respectively, whereas at 5500 MHz, Ants 1, 2, 11 are mainly radiating towards −y, +y, −x directions, respectively. Under LHM condition, as shown in Figs. 15(c) and (d), the proposed MIMO antenna array is now a 2 × 2 MIMO, with Ants 2, 7 radiating towards −y, +y orientation at 3600 MHz, respectively, and Ants 2, 6 radiating towards +y, −y orientation at 5500 MHz, respectively. It is also realized that because Ants 1 and 2 are disposed at the top and bottom right corners of the PCB, they have contributed a lot in radiation and

TABLE 1. Comparison between the proposed and the referenced antennas.

Reference	Bandwidth (GHz)	Efficiency (%)	Ground size (mm^2)	ECC	Peak channel capacity (bps/Hz)	MIMO order
Proposed	3.4–3.8, 5.15–5.925 (–6 dB)	41–82 (low band) and 47–79 (high band)	150 × 80	Lower than 0.15 (low band) and 0.1 (high band)	37 (8 × 8, 20-dB SNR) and 29.5 (6 × 6, 20-dB SNR)	8 (low band) and 6 (high band)
[12]	3.4–3.6 (–6 dB)	59–72	120 × 60	Not mentioned	15 (2 × 8, 20-dB SNR)	8
[13]	3.4–3.8 (–6 dB)	40–57	140 × 70	Lower than 0.1	47 (10 × 10, 20-dB SNR)	10
[15]	3.4–3.6 (–6 dB)	30–53	150 × 75	Lower than 0.3	72 (16 × 16, 20-dB SNR)	16
[17]	3.4–3.6 (–10 dB)	62–78	140 × 70	Lower than 0.2	39 (8 × 8, 20-dB SNR)	8
[14]	2.55–2.65 (–10 dB)	48–63	136 × 68	Lower than 0.15	40 (8 × 8, 20-dB SNR)	8
[19]	3.4–3.6 (–6 dB)	40–52	150 × 75	Lower than 0.15	35 (8 × 8, 20-dB SNR)	8

diversity under data mode. Under RM condition, because Ants 1 and 2 are covered by hand phantom, the open slot antennas will play a major role. As shown in Fig. 15(e), a 6×6 MIMO is observed at 3600 MHz, in which Ants 3, 5, 7, 8, 10, 12 have exhibited maximum radiation oriented in $-$y, $+$x, $+$y, $-$y, $-$x, $+$y directions, respectively. In comparison, as shown in Fig. 15(f), a 4×4 MIMO is observed at 5500 MHz, in which Ants 4, 6, 9, 11 have demonstrated maximum radiation oriented in $-$y, $+$y, $+$y, $-$y directions, respectively. From the above results, under these three mode conditions (RHM, LHM and RM), the radiation patterns of the antenna elements have apparently shown complementary characteristics, which indicates that the proposed MIMO antenna array are still of fairly good diversity performance under data mode and read mode.

Table 1 shows the comparison between the proposed MIMO antenna array and some other massive MIMO antennas reported for mobile handsets. From this Table, it is obvious that the proposed one can support dual-band massive MIMO (LTE band 46 and conventional LTE bands 42/43) with very comparable radiation and MIMO performances. This is a unique feature that all the references do not have.

IV. CONCLUSION

In this paper, a 12-port hybrid antenna array for mobile handsets is proposed and investigated for future 5G/sub-6GHz massive multiple-input multiple-output (MIMO) applications. By integrating all the twelve antenna elements (of three different antenna types, namely, IAs, LAs and SAs), an 8×8 MIMO in long term evolution (LTE) bands 42/43 and 6×6 MIMO in LTE band 46 can be achieved. Good reflection coefficients of better than -6 dB and acceptable isolations of better than -12 dB are achieved. The total efficiency for each antenna element is better than 40% and 45% for LTE bands 42/43 and LTE band 46, respectively. Within the two bands of interest, the envelope correlation coefficient (ECC) value calculated via any two antenna elements is below 0.15, suggesting that the proposed antenna has desirable diversity performance. Furthermore, the calculated ergodic channel capacity levels for the 8×8 MIMO (working in the LTE bands 42/43) and 6×6 MIMO (working in the LTE band 46) are 34–37 bps/Hz and 26.5–29.5 bps/Hz, respectively. The channel capacity results signify that the proposed antenna has much better multiplexing potential than the low-order 2×2 MIMO type. Lastly, the proposed MIMO antenna array is still capable of diversity and multiplexing under the presence of user's hands (data mode and read mode). Therefore, it can be concluded that the proposed MIMO antenna array is very promising for practical 5G multiband MIMO applications.

REFERENCES

[1] S. Zhang, K. Zhao, Z. Ying, and S. He, "Adaptive quad-element multi-wideband antenna array for user-effective LTE MIMO mobile terminals," *IEEE Trans. Antennas Propag.*, vol. 61, no. 8, pp. 4275–4283, Aug. 2013.
[2] J. G. Andrews *et al.*, "What will 5G be?" *IEEE J. Sel. Areas Commun.*, vol. 32, no. 6, pp. 1065–1082, Jun. 2014.
[3] H. Li, Z. T. Miers, and B. K. Lau, "Design of orthogonal MIMO handset antennas based on characteristic mode manipulation at frequency bands below 1 GHz," *IEEE Trans. Antennas Propag.*, vol. 62, no. 5, pp. 2756–2766, May 2014.
[4] H. Elshaer, M. N. Kulkarni, F. Boccardi, J. G. Andrews, and M. Dohler, "Downlink and uplink cell association with traditional macrocells and millimeter wave small cells," *IEEE Trans. Wireless Commun.*, vol. 15, no. 9, pp. 6244–6258, Sep. 2016.
[5] B. Holter, "On the capacity of the MIMO channel: A tutorial introduction," in *Proc. IEEE Norwegian Symp. Signal Process.*, 2001, pp. 167–172.
[6] L. Zheng and D. N. C. Tse, "Diversity and multiplexing: A fundamental tradeoff in multiple-antenna channels," *IEEE Trans. Inf. Theory*, vol. 49, no. 5, pp. 1073–1096, May 2003.
[7] WRC-15 Press Release. (Nov. 27, 2015). *World Radiocommunication Conference Allocates Spectrum for Future Innovation*. [Online]. Available: http://www.itu.int/net/pressoffice/press_releases/2015/56.aspx
[8] Qualcomm. (Sep. 2015). *Making the Best Use of Licensed and Unlicensed Spectrum*. [Online]. Available: https://www.qualcomm.com/media/documents/files/making-the-best-use-of-unlicensed-spectrum-presentation.pdf
[9] IMT-2020 (5G) Promotion Group. (Feb. 2015). *White Paper on 5G Concept*. [Online]. Available: http://www.imt-2020.org.cn/zh/documents/download/4
[10] SK Telecom. (Oct. 2014).*SK Telecom 5G White Paper*. [Online]. Available: http://www.sktelecom.com/img/pds/press/SKT_5G%20White%20Paper_V1.0_Eng.pdf

[11] H. Xu *et al.*, "A compact and low-profile loop antenna with six resonant modes for LTE smartphone," *IEEE Trans. Antennas Propag.*, vol. 64, no. 9, pp. 3743–3751, Sep. 2016.
[12] A. A. Al-Hadi, J. Ilvonen, R. Valkonen, and V. Viikari, "Eight-element antenna array for diversity and mimo mobile terminal in LTE 3500 MHz band," *Microw. Opt. Technol. Lett.*, vol. 56, no. 6, pp. 1323–1327, Jun. 2014.
[13] K.-L. Wong and J. Y. Lu, "3.6-GHz 10-antenna array for mimo operation in the smartphone," *Microw. Opt. Technol. Lett.*, vol. 57, no. 7, pp. 1699–1704, Jul. 2015.
[14] M. Y. Li *et al.*, "Eight-port orthogonally dual-polarized antenna array for 5G smartphone applications," *IEEE Trans. Antennas Propag.*, vol. 64, no. 9, pp. 3820–3830, Sep. 2016.
[15] K. L. Wong, J.-Y. Lu, L.-Y. Chen, W.-Y. Li, and Y.-L. Ban, "8-antenna and 16-antenna arrays using the quad-antenna linear array as a building block for the 3.5-GHz LTE MIMO operation in the smartphone," *Microw. Opt. Technol. Lett.*, vol. 58, no. 1, pp. 174–181, Jan. 2016.
[16] Z. Qin, W. Geyi, M. Zhang, and J. Wang, "Printed eight-element MIMO system for compact and thin 5G mobile handest," *Electron. Lett.*, vol. 52, no. 6, pp. 416–418, Mar. 2016.
[17] Y.-L. Ban, C. Li, C.-Y. D. Sim, G. Wu, and K.-L. Wong, "4G/5G multiple antennas for future multi-mode smartphone applications," *IEEE Access*, vol. 4, pp. 2981–2988, 2016.
[18] K.-L. Wong, C.-Y. Tsai, C.-Y. Lu, D.-M. Chian, and W.-Y. Li, "Compact eight MIMO antennas for 5G smartphones and their MIMO capacity verification," in *Proc. URSI Asia–Pacific Radio Sci. Conf.*, Seoul, South Korea, Aug. 2016, pp. 1054–1056.
[19] K.-L. Wong, C.-Y. Tsai, and J.-Y. Lu, "Two asymmetrically mirrored gap-coupled loop antennas as a compact building block for eight-antenna MIMO array in the future smartphone," *IEEE Trans. Antennas Propag.*, vol. 65, no. 4, pp. 1765–1778, Apr. 2017.
[20] K. L. Chung and S. Chaimool, "Triple-band CPW-FED L-shaped monopole antenna with small ground plane," *Microw. Opt. Technol. Lett.*, vol. 53, no. 10, pp. 2274–2277, Oct. 2011.
[21] S. R. Best, "The significance of ground-plane size and antenna location in establishing the performance of ground-plane-dependent antennas," *IEEE Antennas Propag. Mag.*, vol. 51, no. 6, pp. 29–43, Dec. 2009.
[22] D. Huang, Z. Du, and Y. Wang, "An octa-band monopole antenna with a small nonground portion height for LTE/WLAN mobile phones," *IEEE Trans. Antennas Propag.*, vol. 65, no. 2, pp. 878–882, Feb. 2017.
[23] C.-Y.-D. Sim, C.-C. Chen, X. Y. Zhang, Y.-L. Lee, and C.-Y. Chiang, "Very small-size uniplanar printed monopole antenna for dual-band WLAN laptop computer applications," *IEEE Trans. Antennas Propag.*, vol. 65, no. 6, pp. 2916–2922, Jun. 2017.
[24] H. Y. Wang and H. L. Xu, "Resonant structures and applications to mobile handset antennas," in *Proc. IEEE-APS Topical Conf. Antennas Propag. Wireless Commun.*, Cairns, QLD, Australia, Sep. 2016, pp. 44–46.
[25] H. Wang, D. Zhou, L. Xue, S. Gao, and H. Xu, "Mode analysis and excitation of slot antennas," in *Proc. Loughborough Antennas Propag. Conf.*, Loughborough, U.K., Nov. 2015, pp. 1–4.
[26] H. Wang, "Planar inverted-F antenna and quarter wavelength slot antenna," in *Proc. Asia–Pacific Conf. Antennas Propag.*, Harbin, China, Jul. 2014, pp. 523–525.
[27] M. S. Sharawi, "Printed multi-band MIMO antenna systems and their performance metrics [wireless corner]," *IEEE Antennas Propag. Mag.*, vol. 55, no. 5, pp. 218–232, Oct. 2013.
[28] R. Tian, B. K. Lau, and Z. Ying, "Multiplexing efficiency of MIMO antennas," *IEEE Antennas Wireless Propag. Lett.*, vol. 10, pp. 183–186, 2011.
[29] K. Zhao, S. Zhang, Z. Ying, T. Bolin, and S. He, "SAR study of different MIMO antenna designs for LTE application in smart mobile handsets," *IEEE Trans. Antennas Propag.*, vol. 61, no. 6, pp. 3270–3279, Jun. 2013.
[30] Y. L. Ban, Y. F. Qiang, Z. Chen, K. Kang, and J. H. Guo, "A dual-loop antenna design for hepta-band WWAN/LTE metal-rimmed smartphone applications," *IEEE Trans. Antennas Propag.*, vol. 63, no. 1, pp. 48–58, Jan. 2015.

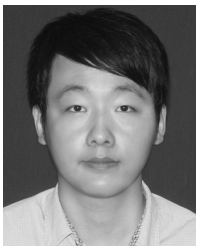

YIXIN LI was born in Hunan, China, in 1994. He received the B.S. degree in communication engineering from Shanghai University, Shanghai, China, in 2016, where he is currently pursuing the M.S. degree in electromagnetic field and microwave technology with the School of Communication and Information Engineering. His current research interests include 5G/sub-6-GHz MIMO antennas for mobile terminals and wireless access points and small antennas embedded in full metal casing.

CHOW-YEN-DESMOND SIM (M'07–SM'13) was born in Singapore, in 1971. He received the B.Sc. degree from the Engineering Department, University of Leicester, U.K., in 1998, and the Ph.D. degree from the Radio System Group, Engineering Department, University of Leicester, in 2003. From 2003 to 2007, he was an Assistant Professor with the Department of Computer and Communication Engineering, Chienkuo Technology University, Chang-Hua, Taiwan. In 2007, he joined the Department of Electrical Engineering, Feng Chia University (FCU), Taichung, Taiwan, as an Associate Professor, where he became a Full Professor in 2012. Since 2016, he has been serving as the Technical Consultant for the Securitag Assembly Group, which is one of the largest RFID tag manufacturers in Taiwan. He is currently serving as the Executive Officer of Master's Program, College of Information and Electrical Engineering (Industrial R&D), the Director of Intelligent IoT Industrial Ph.D. Program. He is the founding Director of the Antennas and Microwave Circuits Innovation Research Center, FCU. He has authored or co-authored over 100 SCI papers. His current research interests include antenna design, VHF/UHF tropospheric propagation, and RFID applications. He is a fellow of the Institute of Engineering and Technology (FIET), a Senior Member of the IEEE Antennas and Propagation Society, and a Life-Member of the IAET. In 2015, he was invited to become the Distinguished Chair Professor (ZhiQian Professor) of the School of Communication and Information Engineering, Shanghai University. He was the TPC member of APMC 2012, APCAP 2015, IMWS-Bio 2015, ISAP 2015, APEMC 2015, CSQRWC 2016, and ICCEM 2017. He has served as the TPC Sub-Committee Chair (Antenna) of ISAP 2014 and PIERS 2017, and the TPC Chair of APCAP 2016. He was invited as the workshop speaker at the APEMC 2015 and the IEEE iAIM 2017. He is currently serving as the Chapter Chair for the IEEE AP-Society, Taipei Chapter (2016–2018). He was a recipient of the IEEE Antennas and Propagation Society Top 10 Outstanding Reviewer Award for Year (2013/2014) and (2014/2015), (2015/2016), and (2016/2017). He is also serving as the Associate Editor for the IEEE AWPL, the IEEE Access, and the *International Journal of RF and Microwave Computer-Aided Engineering*.

YONG LUO received the Ph.D. degree from the the University of Tokyo, with a focus on active metamaterials for scanning radiation beams by using micro-machining fabrication process to monolithically integrate antenna with MEMS. From 2010 to 2012, he was with Huawei as an Electrical Engineer in phased array antennas for base stations. He held a post-doctoral position with Prof. Sievenpiper's Applied Electromagnetic Group in the field of non-linear meta-surfaces using diodes in 2016. He is currently an Assistant Professor with the Department of Electronic and Information Engineering, School of Communication and Information Engineering, Shanghai University. His research interests include active antennas, non-linear metamaterial, and RF-MEMS.

GUANGLI YANG (M'06) received the B.S. degree in physics from the Beijing University of Science and Technology, China, in 1997, and the Ph.D. degree in electrical engineering from the University of South Carolina, USA, in 2005. He was with the Antenna and RF Research Group, Motorola Inc., USA, from 2005 to 2013 started as a Senior, a Senior Staff, and promoted as a Principal Engineer. He has been a Professor with Shanghai University since March 2014. He has authored or co-authored over 60 publications and has over 21 patents filed or issued. His research interests include smart antennas, antenna miniaturization and configurability, digital beam-forming system, and microwave circuits. He is the Director of the RF Research Group, Shanghai University. He was a recipient of the Shanghai "1000 Plan" and "Eastern Scholarship" Awards in 2013.